Mapping the Targeted Membrane Pore Formation Mechanism by Solution NMR: The Nisin Z and Lipid II Interaction in SDS Micelles

Shang-Te Hsu,[‡] Eefjan Breukink,[§] Ben de Kruijff,[§] Robert Kaptein,[‡] Alexandre M. J. J. Bonvin,[‡] and Nico A. J. van Nuland*,[‡]

Department of NMR Spectroscopy, Bijvoet Center for Biomolecular Research, and Department of Biochemistry of Membranes, Center for Biomembranes and Lipid Enzymology, Institute for Biomembranes, Utrecht University, 3584CH Utrecht, The Netherlands

Received February 14, 2002; Revised Manuscript Received April 9, 2002

ABSTRACT: Nisin is an example of type-A lantibiotics that contain cyclic lanthionine rings and unusual dehydrated amino acids. Among the numerous pore-forming antimicrobial peptides, type-A lantibiotics form an unique family of post-translationally modified peptides. Via the recognition of cell wall precursor lipid II, nisin has the capacity to form pores against Gram-positive bacteria with an extremely high activity in the nanomolar (nM) range. Here we report a high-resolution NMR spectroscopy study of nisin/lipid II interactions in SDS micelles as a model membrane system in order to elucidate the mechanism of molecular recognition at residue level. The binding to lipid II was studied through $^{15}N-^{1}H$ HSQC titration, backbone amide proton temperature coefficient analysis, and heteronuclear $^{15}N\{^{1}H\}-NOE$ relaxation dynamics experiments. Upon the addition of lipid II, significant changes were monitored in the N-terminal part of nisin. An extremely low amide proton temperature coefficient ($\Delta\delta/\Delta T$) was found for the amide proton of Ala3 (> -0.1 ppb/K) in the complex form. This suggests tight hydrogen bonding and/or isolation from the bulk solvent for this residue. Large chemical shift perturbations were also observed in the first two rings. In contrast, the C-terminal part of nisin was almost unaffected. This part of the molecule remains flexible and solvent-exposed. On the basis of our results, a multistep pore-forming mechanism is proposed. The N-terminal part of nisin first binds to lipid II, and a subsequent structural rearrangement takes place. The C-terminal part of nisin is possibly responsible for the activation of the pore formation. In light of the emerging antibiotic resistance problems, an understanding of the specific recognition mechanism of nisin with lipid II at the residue specific level may therefore aid in the development of novel antibiotics.

Nisin Z is a 34-residue peptide, which is produced by and primarily acts against Gram-positive bacteria. It belongs to the type-A lantibiotics (lanthionine-containing antibiotics) family (*1*). The common features of lantibiotics are the unique post-translationally modified amino acids dehydroalanine (Dha), dehydrobutyrine (Dhb), and the lanthionine rings that are formed by thioether bonds. Typical type-A lantibiotics are elongated, flexible, and amphipathic peptides that possess pore-forming abilities. In contrast, type-B lantibiotics are compact, globular, and hydrophobic peptides, some of which kill bacteria by blocking the cell wall synthesis pathway (*2*). Nisin Z contains three positively charged lysine residues and five intramolecular lanthionine rings named ring A, B, C, D, and E (Figure 1A). Nisin Z differs from its natural variant nisin A only by a single residue at position 27, a histidine instead of an asparagine, without change in bacterial activity (*3*). In the following, we will refer to nisin Z simply as nisin unless specific comparisons between nisin A and nisin Z are discussed.

The pore-forming function of nisin has been studied in various model membrane systems in vitro by vesicle binding, carboxyflurescein (CF) leakage, potassium ion leakage experiments (for review, see ref *1*), and solid-state nuclear magnetic resonance (NMR) spectroscopy (*4*). High-resolution NMR solution structures of nisin A have been determined in water (*5*) and in the membrane-mimicking environments

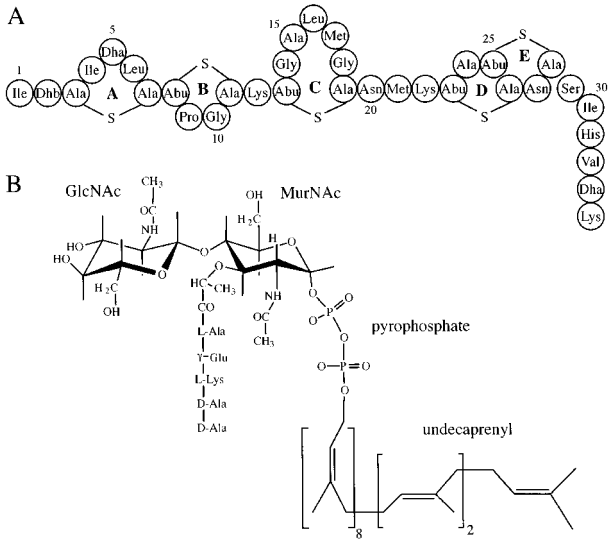

FIGURE 1: Primary structure of nisin Z and lipid II. (A) Dha (U), dehydroalanine; Dhb (O), dehydrobutyrine; Ala−S−Ala (A−S−A), lanthionine; Abu−S−Ala (A*****−S−A), β-methyllanthionine. (B) GlcNAc, *N*-acetylglucosamine; MurNAc, *N*-acetylmuramic acid.

* Corresponding author. Tel: +31-30-2533295. Fax: +31-30-2539254. E-mail: nuland@nmr.chem.uu.nl.

[‡] Bijvoet Center for Biomolecular Research.

[§] Center for Biomembranes and Lipid Enzymology.

10.1021/bi025679t CCC: $22.00
Published on Web 05/24/2002

of dodecylphosphocholine (DPC) and sodium dodecylsulfate (SDS) solutions (*6*). These studies showed a very flexible, extended structure, with rather well-defined local ring substructures. The orientation of nisin on the membrane surface was also studied by fluorescence (*7*), solution NMR (*8*), and solid-state NMR (*4*, *9*). The amphipathic nature of nisin provides a preferential orientation on the membrane interface: both N- and C-terminal parts of nisin were found to be involved in membrane binding; nevertheless, the N-terminal part is more deeply inserted into the membrane (*7*, *8*). Unlike the highly specific activity (nM range) obtained from in vivo studies, the activities of nisin that were previously obtained from in vitro experiments were only in the micromolar (μM) range.

This discrepancy has recently been solved by the discovery that lipid II (Figure 1B), the membrane-bound peptidoglycan precursor for cell wall synthesis, is used as a receptor/docking molecule by nisin (*10*, *11*). The recognition of lipid II facilitates and enhances the pore-forming function of nisin in vitro by a factor of 10^3 in model membrane systems (*11*, *12*). Lipid II is the key element for the synthesis of the protective cell wall for bacteria. The undecaprenyl tail of lipid II acts as a carrier, which transports the peptidoglycan subunit from the cytoplasm to the extracellular domain. Because of the importance of lipid II in the bacterial cell wall synthesis pathway, it is also an unique target for some antibiotics, e.g., vancomycin (*13*). The addition of vancomycin inhibits the activity of nisin in the presence of lipid II, but the binding motif of lipid II for nisin is probably different to that of vancomycin (*11*). However, the exact binding mechanism for nisin is still unclear. The discovery of the specific and high-affinity interaction between nisin and lipid II provides the first known example of targeted pore formation. The results suggest that nisin, or derivatives of it, could one day be used as an alternative antibiotic to overcome the emerging antibiotic resistance problems. The nisin/lipid II interaction is also a useful model system to understand this novel pore-forming mechanism and to provide a blueprint for further peptide engineering and antibiotics development. The elucidation at a structural level of the targeted pore-forming mechanism will be the most comprehensive approach.

Here we present a NMR study of the interaction between nisin and lipid II in SDS micelles as a membrane mimic environment. Various types of high-resolution NMR experiments have been performed to provide insight into the binding mechanism at residue level. We will show that only the N-terminal part of nisin strongly interacts with lipid II, whereas the C-terminal part remains unaffected by the formation of the complex. These results suggest that the pore-forming mechanism is a multistep process in which nisin possesses different functionalities throughout several segments: (i) initial recognition of the N-terminal part followed by subsequent aggregation and (ii) at the later stage, activation of the pore formation by the C-terminal part.

MATERIALS AND METHODS

Sample Preparation. ^{15}N-labeled nisin Z was isolated and purified as described (*14*) using a ^{15}N-enriched growth medium as nitrogen source, and lipid II was prepared as described (*15*). Nisin was dissolved in 500 μL of 10% D_2O and 90% H_2O, with 25 mM sodium phosphate buffer adjusted to pH 6.0, resulting in sample concentrations of 1.8 mM for the unlabeled peptide and 1 mM for the ^{15}N-labeled peptide. 4% and 2% perdeuterated d_{25}-SDS were added into the unlabeled and ^{15}N-labeled samples, respectively, to bring the SDS concentration to approximately 100 fold excess with respect to the peptide concentration. Since the 1D NMR spectrum showed no significant changes when the nisin-to-SDS ratio was changed from 1:20 to 1:60 (*16*), further changes were therefore solely due to the incorporation of lipid II. This also ensured a ratio of approximately one peptide per micelle in order to form a 1:1 complex with lipid II.

NMR Spectroscopy and Titration Experiments. NMR spectra were recorded on Varian INOVA 750 and 500 MHz spectrometers. 2D NOESY (*17*) with mixing times of 100, 150, and 200 ms and 2D clean-TOCSY (*18*) with mixing times of 60 and 100 ms were performed for the backbone resonance assignment of nisin in SDS solution with and without the presence of lipid II. All 2D spectra were recorded with 2048 complex *t2* points and 1024 complex *t1* points. 3D ^{15}N NOESY−HSQC (*19*) and ^{15}N TOCSY−HSQC with DIPSI-2 spin-lock sequence (*20*) were recorded with mixing times of 100 and 60 ms, respectively. For both 3D experiments, the spectra size was set to 1600*280*144 complex points for the direct ^{1}H dimension and the indirect ^{1}H and ^{15}N dimensions, respectively. In the ^{15}N-^{1}H HSQC titration experiments, 25 μL of 3mM lipid II in 2% d_{25}-SDS was added successively five times into 400 μL of 0.75 mM ^{15}N-labeled nisin. This led to 24% dilution of the nisin concentration at the final step and a final molar ratio of nisin to lipid II of 1:1.25. ^{15}N−^{1}H HSQC spectra (*21*) were recorded with 1600 complex *t2* points and 180 complex *t1* points. All spectra were recorded at 20 °C with the WATERGATE water suppression protocol (*22*). Steady-state heteronuclear ^{15}N{^{1}H}-NOE experiments with and without saturation irradiation during the 3 s relaxation delay period were recorded on the nisin/lipid II complex at 40 °C as described previously (*23*). The spectra size was the same as in the titration experiments. For amide proton temperature coefficient measurements, ^{15}N−^{1}H HSQC spectra were recorded at 10, 20, 30, and 40 °C. Additional 2D and 3D NOESY experiments were performed at 40 °C on the nisin/lipid II complex after titration. All spectra were processed with the NMRPIPE software package (*24*) and analyzed with NMRView (*25*).

RESULTS

Backbone Resonance Assignments of Nisin Z. Although the small sequence difference of nisin Z from its natural variant, nisin A (H27N), does not affect its bacterial activity (*3*), its backbone resonances in SDS micelles turned out to be rather different. Apparently, the difference in pH (for nisin A, pH 2.1 (*16*) and 3.5 (*26*); for nisin Z in our current report, pH 6) affects the chemical shifts substantially. This is unlikely caused by the single-residue variation, H27N, which would probably only induce localized chemical shift changes due to the difference in electrostatic interaction. The backbone assignment of nisin Z in SDS solution was performed using the standard sequential assignment procedure by combination of ^{15}N NOESY−HSQC and ^{15}N TOCSY−HSQC spectra, except for the residues flanked by two glycine residues, i.e., Ala15, Leu16, and Met17, in ring C. During

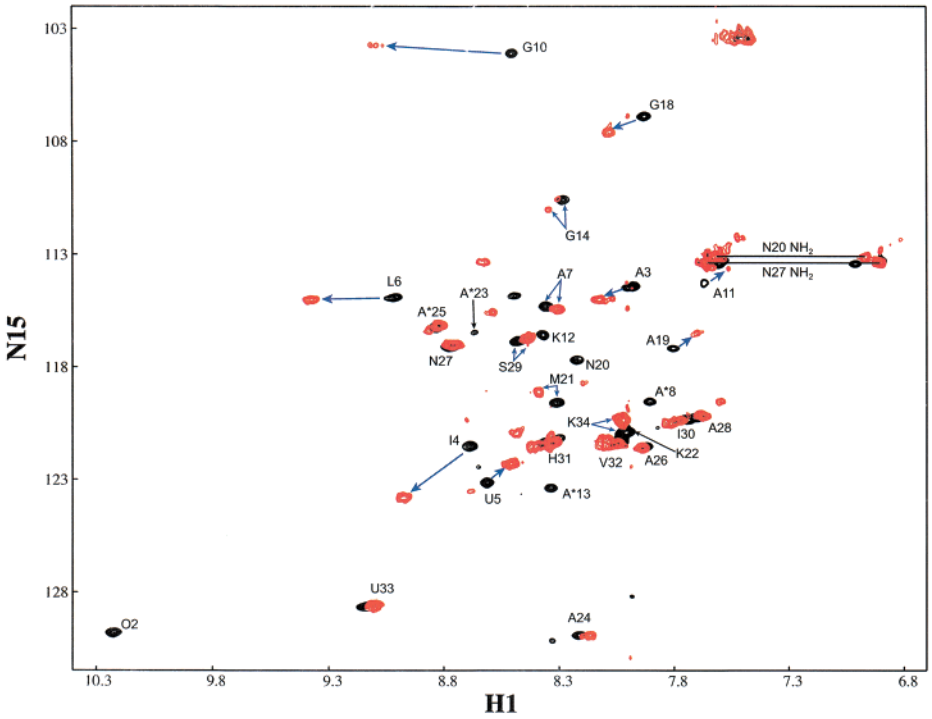

FIGURE 2: $^{15}N-^{1}H$ HSQC titration spectra of ^{15}N-labeled nisin before (black) and after the addition of lipid II (red). The red cross-peaks correspond to a molar ratio of nisin/lipid II of 1:1.25. Residues undergoing large or obvious chemical shift perturbations are indicated by blue arrows. The unlabeled cross-peaks could not be assigned due to the lack of signals in the TOCSY and NOESY spectra. A*8, K12, A*13, N20, and K22 could only be assigned in the free form (see text for details).

the titration of lipid II, many residues showed slow exchange binding patterns. At the final step of the titration, a similar sequential assignment approach was attempted; however, only few residues were clearly resolved. Most residues showed weak NOE cross-peaks that hampered the complete assignment of nisin in the lipid II-bound form. For those residues that did not show significant shift upon complexation, mainly in the C-terminal part, the assignments were taken from the free form. These assignments were confirmed by the similarity in the spin system patterns in the NOESY spectrum. The backbone amide proton NOE connectivity $HN_{(i-1)}-HN_{(i)}$ was initially used for the sequential assignments of those residues that showed large chemical shift perturbations. They were then checked by comparison of the spin system patterns. Figure 2 shows the assigned HSQC spectrum of nisin in the free and the lipid II-bound form. Note that there are still some unassigned residues because of the lack or the low intensity of NOE signals.

Lipid II Titration Experiments Show Strong Binding Affinity. The titration of lipid II to ^{15}N-labeled nisin in the presence of SDS shows that the binding is in the slow exchange regime. Several residues undergo large chemical shift perturbation and show typical slow exchange sets of peaks corresponding to the free and the bound form. These peaks coexist during the titration process until 25% excess of lipid II is added, after which all nisin molecules are in the complex form. According to the titration profile, the stoichiometry corresponds to a 1:1 nisin to lipid II complex (data not shown). Figure 3 shows the chemical shift changes upon binding as a function of the nisin sequence. The largest changes are observed in the first three N-terminal ring systems, especially Ile4, Leu6, and Gly10. The chemical shifts of the C-terminal part of nisin, starting from Ala24 up to Lys34, are hardly affected upon the addition of lipid II. We were not able to complete the assignment of the HSQC spectrum at the last point of the titration study; some peaks disappeared due to line broadening after 50% addition of lipid II, and some peaks showed overlap. In contrast to the fast exchange process, in which the average signals of the bound and the free forms can be easily followed during the titration steps, it was not possible to track the chemical shifts in the slow exchange regime. This is particularly the case for Lys12 and Asn20, for which no suitable cross-peaks close to the original positions could be identified. These missing peaks possibly overlap with others or simply disappear due to line broadening. The cause of line broadening is most likely due to slow conformational rearrangement of the relative orientations of the ring systems. Other residues such as Ile4, Leu6, and Gly10 shifted by more than 0.3 ppm downfield along the ^{1}H dimension (Figure 3A), suggesting that rings A and B are in the vicinity of the nisin/lipid II interface. These large downfield shifts are most likely caused by the deshielding effect upon the formation of intra or intermolecular hydrogen bonds with lipid II.

Amide Proton Temperature Coefficients and Solvent Accessibility. Hydrogen bond formation can stabilize the exchangeable backbone amide protons and therefore reduce the exchange rate with the bulk solvent. The stability can also arise from the reduction of solvent accessibility, such as the burial into the complex interface. The amide proton temperature coefficient analysis has been performed to verify whether the largest chemical shift changes of nisin in the titration experiment are indeed due to hydrogen bond formation or due to exclusion from solvent. The temperature dependency of amide proton chemical shifts is a simple probe that provides information on the involvement in hydrogen bond formation or sequestering from the solvent (*27*). A low dependency of the amide chemical shift on temperature in

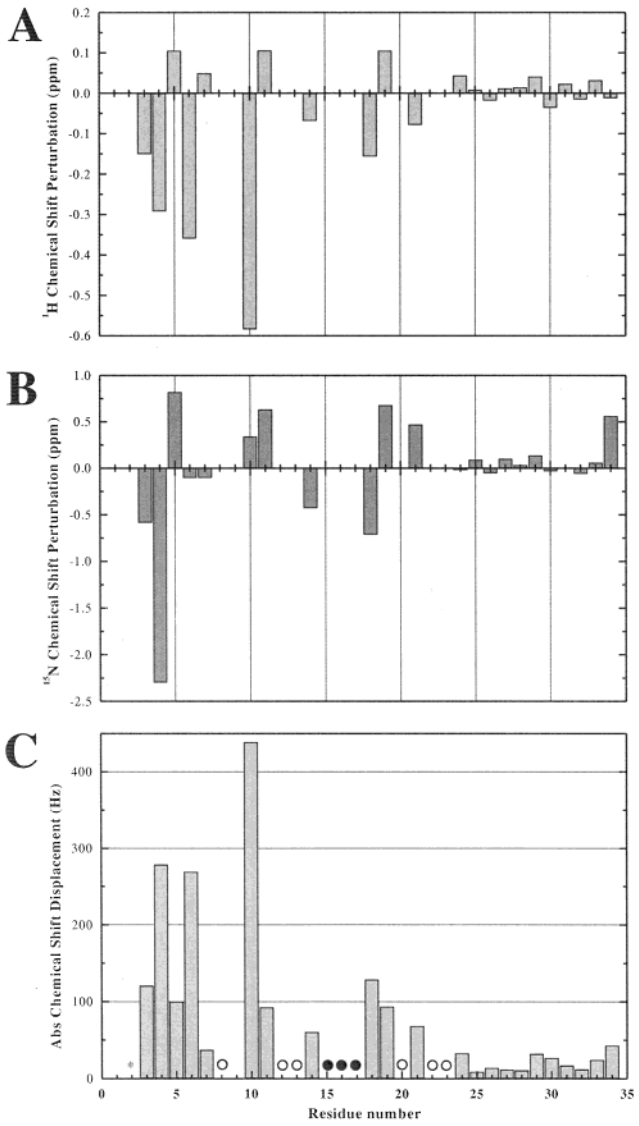

FIGURE 3: Chemical shift perturbation along the sequence of nisin upon the addition of lipid II. (A) ^{1}H chemical shift perturbations are displayed as the difference in chemical shift between the free and the bound forms, respectively, $\Delta\delta_{HN} = \delta_{HN}^{nisin} - \delta_{HN}^{nisin/lipidII}$. (B) ^{15}N chemical shift perturbations $\Delta\delta_N = \delta_N^{nisin} - \delta_N^{nisin/lipidII}$. (C) Absolute chemical shift displacements in Hz. The values are calculated as $[(\Delta\delta_{HN})^2 + (\Delta\delta_N)^2]^{1/2}$ from spectra recorded at 750 MHz. Dhb2 is labeled with an asterisk (*) for the loss of signal after the addition of lipid II. Closed circles (●): unassigned residues in the absence of lipid II due to spectral overlap or ambiguities. Open circles (○): unassigned residues in the complex form.

aqueous environment, i.e., temperature coefficient $\Delta\delta/\Delta T > -2.5$ ppb/K, is usually indicative of the presence of a stable hydrogen bond. For solvent-accessible amide protons, which are more sensitive to a temperature change, the slope is generally more negative than −5 ppb/K (*28*, *29*). We have collected several ^{15}N−^{1}H HSQC spectra of the nisin/lipid II complex under different temperatures ranging from 10 to 40 °C. Figure 4 shows the temperature coefficients of nisin and examples of the amide chemical shift change for some of the residues. While the amide proton chemical shift of Ala3 hardly changes upon temperature increase, Ala7 and Ser29 are more strongly affected. On the basis of the above criteria, the stable amide protons with low solvent accessibility either via hydrogen bond formation or structurally

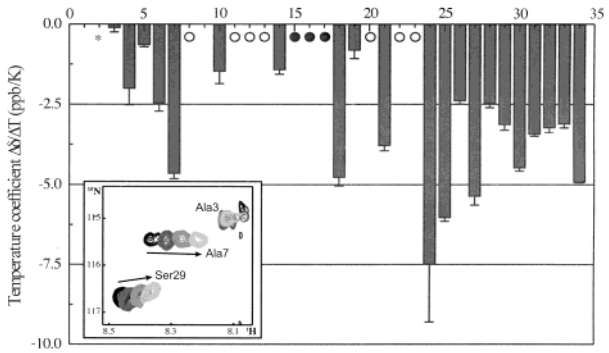

FIGURE 4: Amide proton temperature coefficients ($\Delta\delta/\Delta T$) of nisin in the complex form. The temperature coefficients were obtained by linear fitting of the amide chemical shift δ_{HN} as a function of the temperature measured at 10, 20, 30, and 40 °C. The fitting errors are indicated by bars. The unassigned residues are labeled as described in Figure 3. Inset: representative region of ^{15}N−^{1}H HSQC spectra of nisin in the complex. The cross-peaks are colored in gray scale from black (10 °C) to light gray (40 °C). The direction of the change of the cross-peak position of each residue as a function of temperature is indicated by an arrow. Note that Ala3 is almost unaffected throughout a wide temperature range.

protected from the solvent exchange process are identified for Ala3, Ile4, Dha5, Gly10, Gly14, and Ala19.

Dynamic Properties of Nisin/Lipid II Complex. Unlike most proteins that possess rigid and well-defined globular structures, nisin shows flexibility that is functionally important. This creates, however, a major challenge for our current NMR study: the dynamics results in an averaging of structural information, which makes a characterization of the complex difficult. Steady-state heteronuclear ^{15}N{^{1}H}-NOE experiments have been performed on the nisin/lipid II complex to investigate its dynamic properties. The heteronuclear NOE is a very sensitive probe for fast backbone motion in the picosecond to nanosecond time scale (*30*−*32*). It gives a measure of the rigidity of the backbone and is defined as the ratio of peak intensities with and without saturation irradiation. Well-defined and rigid structure elements usually give positive NOEs close to unity. In the nisin/lipid II complex at 40 °C, negative NOEs were obtained for Dha33 and Lys34 and either weak or zero NOEs for residues 30−32: evidence of a highly dynamic motion. In contrast, the N-terminal part was relatively rigid, showing positive NOEs (data not shown). These results demonstrate that two different dynamic properties are distributed along the nisin sequence. These findings are in agreement with the chemical shift perturbation and amide temperature coefficient analysis and confirm that the C-terminal part of the molecule is not involved in the binding of lipid II.

DISCUSSION

In the present report, we have provided a residue specific analysis of nisin/lipid II interactions in a model membrane system by solution NMR spectroscopy. Figure 5 summarizes the results of the HSQC titration experiment and amide proton temperature coefficient analysis. It should be noted that the observed chemical shift changes of nisin upon the addition of lipid II could in principle arise from either the direct interactions of the affected residues with lipid II or the indirect effect from changes in nisin-SDS interactions on forming the complex. The incorporation of lipid II has the potential to induce a morphological change of SDS

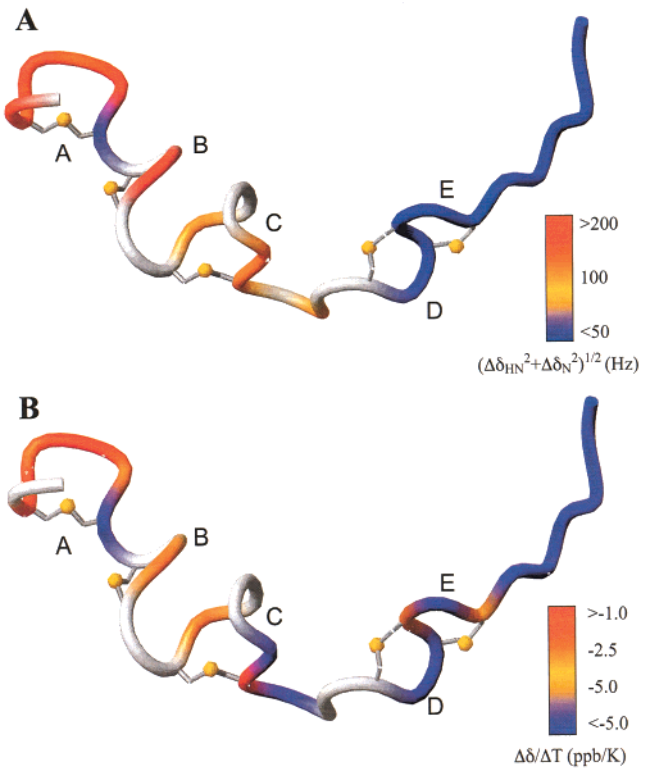

FIGURE 5: Mapping of the lipid II titration and the temperature dependency results onto the nisin structure. (A) The chemical shift perturbations after the addition of lipid II to nisin. The color coding is based on the absolute chemical shift displacements in Figure 3C. The unassigned residues are colored in white. (B) The temperature dependency of nisin in the complex form with nisin. The thioether linkages are shown in ball-and-stick representation, with the yellow sulfur atoms. The ring systems of nisin are labeled from A to E according to the definition in Figure 1A. The nisin coordinates correspond to the representative structure of nisin in the presence of DPC micelles (*6*). These were kindly provided by Dr. H. W. van den Hooven. The figures were generated by MOLMOL (*42*).

micelles and therefore change the mode of interaction between nisin and micelle surface. It has been demonstrated that the difference in the surface curvatures of different membrane mimicing media, e.g., micelles and bicelles, can induce subtle backbone conformational changes of membrane interacting peptides (*33*). These structural differences are clearly reflected by substantial changes in the $^1H-^{15}N$ HSQC spectra. In our case, however, no peak shift was observed during the titration process; only the signal population decreases at the free form position and increases at the bound form position until all nisin molecules are bound to lipid II. This suggests that lipid II integrates into SDS micelles and interacts with nisin in such a way that only the lipid II bound micelles are affected and the state of the lipid II-free micelles remains the same. A previous SDS titration study of nisin in the absence of lipid II has shown that the progressive excess of SDS concentration, which could also result in larger micelle size, does not change the spectrum of nisin after the nisin-to-SDS ratio reaches 1:20 (*16*). This suggests that the conformation of nisin is not sensitive to the morphology of SDS micelles. Although hampered by the lack of intermolecular NOE data from the nisin/lipid II complex, all data strongly support the idea that the addition of lipid II induces a substantial chemical environment change of the N-terminal part of nisin mainly through direct binding. The interaction of nisin with SDS micelles is therefore changed simultaneously. The micelle morphology may alter due to the insertion of lipid II, although this effect is relatively minor.

Although the nature of the flexibility of nisin at higher pH leaves some unassigned residues in our current study, studies at high pH (>pH 5) are required since at pH 3−4 the nisin/lipid II complex is not formed according to circular dichroism (CD) spectroscopy studies (data not shown). In the absence of lipid II, the secondary structure of nisin in SDS micelles monitored by CD spectroscopy does not change significantly between pH 5 and 8. In contrast, it is very sensitive to the pH changes in aqueous solution. Despite the relative small amplitude of absorption, the spectral patterns of nisin in SDS micelles at pH 3 and 4 are still similar to those at higher pH (*34*). All of this evidence suggests that the conformation of nisin is relatively stable once it is in SDS micelle solution. The difference in pH in the sample condition and the single variant H27N might be the reason for the discrepancy between our result and the previous studies of the chemical shift assignments. Nevertheless, the effect of the binding to lipid II is significant, and the 1:1 stoichiometry obtained from the lipid II titration profile in SDS micelles confirms the proposed stoichiometry obtained from the direct binding assay (*11*).

N-Terminal Part of Nisin Is Responsible for the First Recognition Step. The binding to lipid II perturbs mainly the chemical shifts of residues localized in the first two rings, A and B. The specific binding process is in the slow exchange regime, and some residues show large chemical shift changes, for example, Ile4, Leu6 and Gly10. Some residues, however, show broad lines in the free and/or in the complex form, mostly those in ring C and the following hinge region. This probably reflects some structural inhomogeneity in this part of the molecule.

The complex formation also enhances the stability of several backbone amide protons in the N-terminal part of the structure, as has been demonstrated by the temperature coefficient analysis. The extremely small amide proton temperature coefficient of Ala3 (> −0.1 ppb/K) suggests that it is highly protected from the exchange process with the bulk solvent. The downfield shifting of the amide protons in rings A and B in the ^1H dimension can be explained by the deshielding effect due to the involvement in a hydrogen bond network in the complex structure. For Dha5, although slightly upfield shifted upon binding, its amide proton might be already protected prior to the complex formation so that no additional stability enhancement is observed. It is therefore reasonable to hypothesize that the first three rings, mainly rings A and B, form a binding pocket and bind tightly to lipid II. An interesting aspect in this study, compared with the previous report in aqueous solution, SDS and DPC micelles is that the binding of lipid II particularly reduces the amide proton temperature coefficients of the amide protons of rings A and B approximately 2-fold (those of nisin A in SDS micelles are about −4 to −8 ppb/K throughout the sequence except Dha5 and Ala11; *8*). Nevertheless, care should be taken in the comparison since our sample pH value is different from the previous study. Despite the difference in pH condition, a dramatic change of the temperature coefficient from about −7 to −0.1 ppb/K is observed for Ala3, while the C-terminal part of nisin is roughly unaffected (generally < −4 ppb/K). This suggests that the complex

interface is formed by the N-terminal part of nisin and lipid II and therefore results in the low solvent accessibility particularly in this part of nisin.

We also note the excellent correlation among the chemical shift perturbation, amide proton temperature coefficient analysis, and relaxation studies: they all indicate the same structural behavior along the sequence of nisin, with the hinge region defining the border between these structural elements. The C-terminal part of nisin, starting from rings D and E, does not seem to interact with lipid II. Although the backbone geometry of these two intertwined rings is tightly confined by the thioether linkages, the corresponding backbone amide protons are still highly solvent accessible and show high mobility. This indicates that these two rings are neither buried into the SDS micelles nor complexed with lipid II. Our observations suggest that only the N-terminal part of nisin is responsible for the recognition of lipid II, the C-terminal part being probably more important for the pore formation at a later stage. This model is supported by two other studies: (i) the N-terminal fragment nisin$^{1-12}$ can act as an antagonist to inhibit the bacterial activities of the full-length nisin (*35*), and (ii) the introduction of a positively charged lysine at position 32 (V32K) does not seriously disrupt nisin activity in the presence of lipid II (*12*).

Recently, Wiedemann and co-workers have performed a series of mutagenesis studies, which have pinpointed out the importance of the structures of the lanthionine rings A and C and of the flexibility of the hinge region for the binding to lipid II and the pore formation (*12*). From these studies, it has been shown that there exists a high structural selectivity at position 3 (Ala3) while the preceding position (Dhb2) has more tolerance. Introduction of an extra methyl group at position 3 of the prepeptide (S3T) changes the lanthionine linkage to a 3-methyllanthionine, and this substantially reduces its activity (MIC for *M. flavus*: S3T = 39 nM vs wild type = 3.3 nM), while the modification of Dhb2 into other residue types is less significant. In addition, hydrolytic cleavage at Dha5, by which the ring A is opened, results in substantial loss of biological activity, whereas the same cleavage at Dha33, removing the last two residues, has very little effect (*36*, *37*). As discussed above, the low amide proton temperature coefficients and the localized chemical shift perturbations provide the first direct proof of the tight binding and of the increase of stability upon binding of lipid II. This increase could be the result of a highly complimentary binding interface. Any additional chemical modification at this position would abolish the complimentarity and therefore disrupt its activity. In this case, a 3-methyllanthionine causes a structural clash because of the extra methyl group in the ring linkage position, which makes it difficult for nisin to adopt a suitable geometry for the binding of lipid II. The same explanation also applies to Gly14 and Ala19. These two amide protons show similar patterns of chemical shift perturbation and amide proton temperature coefficient during complex formation. This suggests that ring C is also involved in the binding process but maybe to a lesser extent. Our NMR results above have located the binding interface of nisin, essentially rings A and B, and explained the selectivity of residue types obtained from the mutagenesis study, especially for Dhb2 and Ala3 in ring A.

The involvement of ring C has been studied by other mutagenesis studies. The removal of the C-terminal fragment, in which the first 20 residues are kept, nisin$^{1-20}$, increases the MIC value by 10 fold; yet a further removal of ring C, nisin$^{1-12}$, results in more than a 200-fold increase of MIC value (*35*). This suggests that ring C is also important for the growth inhibitory function. Introduction of a charged residue by replacing Met17 to a lysine can abolish the activity by 50%. Furthermore, a single T13C point mutation of the prepeptide, which extends the ring C linkage by replacing the thioether bond to a disulfide bond, results in a mutant which is almost inactive in vivo and in the liposome CF leakage assay (*12*). These results explain the involvement of ring C, in particular Gly14 and Ala19, during the lipid II binding process that were observed in our study.

It is important to note that the dual dynamic property (stable N-terminus vs flexible C-terminus) of nisin can be critical for its bacterial activity. The previously proposed wedge model was based on results obtained in the absence of lipid II. Most of the rings were found to be involved in the membrane binding process (*38*, *39*). Without lipid II, the electrostatic attraction between the positively charged residues of nisin and the negatively charged headgroups of the membrane is dominant. It is therefore no surprise that both termini were found to interact with the model membrane systems in the previous studies; the contributions of the three lysine residues are rather equivalent. The enhancement of activity observed after the incorporation of lipid II, however, indicated that there must exist another dominating interaction between lipid II and nisin. The functional role of the C-terminal part in pore formation is no longer equivalent to that of the N-terminal part. In contrast to the recognition role of the N-terminal part, it is more important for the pore formation at a later stage (*40*).

Hinge Region Bridges the Two Dynamic Structural Elements. In a previous NMR study of nisin A, the hinge region was found to be relatively structured forming a type-II β-turn in the presence of SDS and DPC micelles. This turn is stabilized by backbone hydrogen bonds, in particular between Met21 and Abu24 (*6*). In the case of nisin Z in the presence of lipid II, however, high mobility and/or structural inhomogeneity is still present. This might be functionally important: shortening of the hinge region by the removal of two residues at position 20 and 21 or introduction of proline residues at these positions to enhance rigidity causes a severe loss of the pore-forming activity (*12*). Reduction of flexibility in the hinge region can disable further pore formation by which the translocation of the C-terminal part across the membrane is necessary (*41*). Since there exist two very different dynamic motions along the structure of nisin, the hinge region therefore plays the transitional role to bridge the two termini together. This intermediate motion can also be the reason of the line broadening and the missing peaks in this part of the structure, for example, Asn20.

Aggregation of the Nisin/Lipid II Complex after the Binding Process. Elucidation of the nisin/lipid II complex structure was not possible at this stage due to a dramatic loss of cross-peaks in NOESY spectra. After the titration of lipid II into the nisin/SDS solution, slow aggregation was observed and the increase of size was such that only the C-terminal part of nisin exhibiting high flexibility showed resolvable cross-peaks. Increasing the temperature substantially improved the line widths in the HSQC spectra, but the NOESY spectra were still poor even at the elevated

temperature of 40 °C. Not being able to penetrate SDS gel in the standard electrophoresis experiment, when nisin is bound to lipid II, is also a supplementary indication of the formation of a sizable aggregate (data not shown). This suggests that the subsequent aggregation of the nisin/lipid II complex is essential for the pore formation. The loss of NOE signals after the complex formation is not only due to the slowing down of the molecular tumbling but also to the structural heterogeneity during the aggregation process.

Multistep Lipid II Targeted Pore Formation Mechanism. On the basis of the information in our current study and previously reported mutagenesis results, we propose a multistep model for lipid II-mediated nisin pore formation. The first step involves the recognition of the lipid II headgroup by the N-terminal part of nisin. A tight nisin/lipid II complex is thereby formed, anchored into the membrane by the undecaprenyl tail of lipid II. Subsequent conformational rearrangement takes place by means of the aggregation of the nisin/lipid II complexes. The minimum number of nisin molecules for pore formation is, however, still unclear. Finally, the insertion of the C-terminal part of nisin into the membrane completes the pore-forming process.

Here we have observed the first recognition step in the complete mechanism. The mapping of the binding interface of nisin has provided insight into the functionality of each amino acid along the nisin sequence. The conserved residues among the type-A lantibiotics might also share similar functionalities. We think that the work presented here will benefit to the future studies of this target mediated membrane pore formation mechanism and might aid the future development of novel antibiotics.

ACKNOWLEDGMENT

We thank Dr. R. Wechselberger for expert help with the NMR spectra collection and Dr. C. van Kraaij and R. Bongers from the NIZO food research for their help with the purification of the ^{15}N-labeled nisin.

REFERENCES

1. Breukink, E., and de Kruijff, B. (1999) *Biochim. Biophys. Acta 1462*, 223−234.
2. Brötz, H., and Sahl, H.-G. (2000) *J. Antimicrob. Chemother. 46*, 1−6.
3. Kuipers, O. P., Bierbaum, G., Ottenwalder, B., Dodd, H. M., Horn, N., Metzger, J., Kupke, T., Gnau, V., Bongers, R., van den Bogaard, P., Kosters, H., Rollema, H. S., de Vos, W. M., Siezen, R. J., Jung, G., Götz, F., Sahl, H., and Gasson, M. J. (1996) *Antonie van Leeuwenhoek 69*, 161−170.
4. Bonev, B. B., Chan, W. C., Bycroft, B. W., Roberts, G. C., and Watts, A. (2000) *Biochemistry 39*, 11425−11433.
5. van de Ven, F. J., van den Hooven, H. W., Konings, R. N., and Hilbers, C. W. (1991) *Eur. J. Biochem. 202*, 1181−1188.
6. van den Hooven, H. W., Doeland, C. C., van de Kamp, M., Konings, R. N., Hilbers, C. W., and van de Ven, F. J. (1996) *Eur. J. Biochem. 235*, 382−393.
7. Breukink, E., van Kraaij, C., van Dalen, A., Demel, R. A., Siezen, R. J., de Kruijff, B., and Kuipers, O. P. (1998) *Biochemistry 37*, 8153−8162.
8. van den Hooven, H. W., Spronk, C. A., van de Kamp, M., Konings, R. N., Hilbers, C. W., and van de Van, F. J. (1996) *Eur. J. Biochem. 235*, 394−403.
9. Jastimi, R. E., Edwards, K., and Lafleur, M. (1999) *Biophys. J. 77*, 842−852.
10. Brötz, H., Josten, M., Wiedemann, I., Schneider, U., Götz, F., Bierbaum, G., and Sahl, H.-G. (1998) *Mol. Microbiol. 30*, 317−327.
11. Breukink, E., Wiedemann, I., van Kraaij, C., Kuipers, O. P., Sahl, H.-G., and de Kruijff, B. (1999) *Science 286*, 2361−2364.
12. Wiedemann, I., Breukink, E., van Kraaij, C., Kuipers, O. P., Bierbaum, G., de Kruijff, B., and Sahl, H.-G. (2001) *J. Biol. Chem. 276*, 1772−1779.
13. Sheldrick, G. M., Jones, P. G., Kennard, O., Williams, D. H., and Smith, G. A. (1978) *Nature 271*, 223−225.
14. Kuipers, O. P., Rollema, H. S., Yap, W. M., Boot, H. J., Siezen, R. J., and de Vos, W. M. (1992) *J. Biol. Chem. 267*, 24340−24346.
15. Brötz, H., Bierbaum, G., Reynolds, P. E., and Sahl, H.-G. (1997) *Eur. J. Biochem. 246*, 193−199.
16. van den Hooven, H. W. (1995) Ph.D. Thesis, Katholieke Universteit Nijmegen, Nijmegen, The Netherlands.
17. Jeener, J., Meier, B. H., Bachman, P., and Ernst, R. R. (1982) *J. Chem. Phys. 71*, 4546−4553.
18. Griesinger, C., Otting, G., Wüthrich, K., and Ernst, R. R. (1988) *J. Am. Chem. Soc. 110*, 7870−7872.
19. Marion, D., Driscoll, P. C., Kay, L. E., Wingfield, P. T., Bax, A., Gronenborn, A. M., and Clore, G. M. (1989) *Biochemistry 28*, 6150−6156.
20. Marion, D., Kay, L. E., Sparks, S. W., Torchia, D. A., and Bax, A. (1989) *Biochemistry 111*, 1515−1517.
21. Kay, L. E., Keifer, P., and Saarinen, T. (1992) *J. Am. Chem. Soc. 114*, 10663−10665.
22. Piotto, M., Saudek, V., and Sklenar, V. (1992) *J. Biomol. NMR 2*, 661−665.
23. Meunier, S., Spurio, R., Czisch, M., Wechselberger, R., Guenneugues, M., Gualerzi, C. O., and Boelens, R. (2000) *EMBO J. 19*, 1918−1926.
24. Delaglio, F., Grzesiek, S., Vuister, G. W., Zhu, G., Pfeifer, J., and Bax, A. (1995) *J. Biomol. NMR 6*, 277−293.
25. Johnson, B. A., and Blevins, R. A. (1994) *J. Biomol. NMR 4*, 603−614.
26. Sailer, M., Helms, G. L., Henkel, T., Niemczura, W. P., Stiles, M. E., and Vederas, J. C. (1993) *Biochemistry 32*, 310−318.
27. Cierpicki, T., and Otlewski, J. (2001) *J. Biomol. NMR 21*, 249−261.
28. Ballardin, A., Fischman, A. J., Gibbons, W. A., Roy, J., Schwartz, I. L., Smith, C. W., Walter, R., and Wyssbrod, H. R. (1978) *Biochemistry 17*, 4443−4454.
29. Graham, W. H., Carter, E. S., II, and Hicks, R. P. (1992) *Biopolymers 32*, 1755−1764.
30. Kay, L. E., Torchia, D. A., and Bax, A. (1989) *Biochemistry 28*, 8972−8979.
31. Kay, L. E. (1998) *Nat. Struct. Biol. 5 Suppl*. 513−517.
32. Pamler, A. G., III. (2001) *Annu. Rev. Biophys. Biomol. Struct. 30*, 129−155.
33. Chou, J. J., Kaufman, J. D., Stahl, S. J., Wingfield, P. T., and Bax, A. (2002) *J. Am. Chem. Soc. 124*, 2450−2451.
34. Dykes, G. A., Hancock, R. E. W., and Hastings, J. W. (1998) *Biochem. Biophys. Res. Comm. 247*, 723−727.
35. Chan, W. C., Leyland, M., Clark, J., Dodd, H. M., Lian, L. Y., Gasson, M. J., Bycroft, B. W., and Roberts, G. C. K. (1996) *FEBS Lett. 390*, 129−132.
36. Chan, W. C., Bycroft, B. W., Lian, L. Y., and Roberts, G. C. K. (1989) *FEBS Lett. 252*, 29−36.
37. Chan, W. C., Dodd, H. M., Horn, N., Maclean, K., Lian, L. Y., Bycroft, B. W., Gasson, M. J., and Roberts, G. C. K. (1996) *Appl. Environ. Microbiol. 62*, 2966−2969.
38. Driessen, A. J., van den Hooven, H. W., Kuiper, W., van de Kamp, M., Sahl, H.-G., Konings, R. N., and Konings, W. N. (1995) *Biochemistry 34*, 1606−1614.
39. Moll, G. N., Roberts, G. C. K., Konings, W. N., and Driessen, A. J. M. (1996) *Antonie Van Leeuwenhoek 69*, 185−191.
40. van Heusden, H., de Kruijff, B., and Breukink, E. Manuscript in preparation.
41. van Kraaij, C., Breukink, E., Noordermeer, M. A., Demel, R. A., Siezen, R. J., Kuipers, O. P., and de Kruijff, B. (1998) *Biochemistry 37*, 16033−16040.
42. Koradi, R., Billeter, M., and Wüthrich, K. (1996) *J. Mol. Graphics 14*, 51−55.

BI025679T